Regular Article

blood

IMMUNOBIOLOGY AND IMMUNOTHERAPY

Novel nonsense gain-of-function *NFKB2* mutations associated with a combined immunodeficiency phenotype

Hye Sun Kuehn,[1] Julie E. Niemela,[1] Karthik Sreedhara,[1] Jennifer L. Stoddard,[1] Jennifer Grossman,[2] Christian A. Wysocki,[3] M. Teresa de la Morena,[3] Mary Garofalo,[4] Jingga Inlora,[5] Michael P. Snyder,[5] David B. Lewis,[6] Constantine A. Stratakis,[7-9] Thomas A. Fleisher,[1] and Sergio D. Rosenzweig[1]

[1]Immunology Service, Department of Laboratory Medicine, Clinical Center, National Institutes of Health (NIH), Bethesda, MD; [2]Division of Hematology and Hematologic Malignancies, Alberta Health Services, Calgary, AB, Canada; [3]Division of Allergy and Immunology, Department of Internal Medicine and Pediatrics, University of Texas Southwestern Medical Center, Dallas, TX; [4]Laboratory of Host Defenses, National Institute of Allergy and Infectious Diseases, NIH, Bethesda, MD; [5]Department of Genetics and [6]Division of Allergy, Immunology, and Rheumatology, Department of Pediatrics, Stanford University School of Medicine, Stanford, CA; and [7]Section on Endocrinology and Genetics, [8]Program on Developmental Endocrinology and Genetics, and [9]Pediatric Endocrinology Inter-institute Training Program, Eunice Kennedy Shriver National Institute of Child Health and Human Development, NIH, Bethesda, MD

Key Points

- *NFKB2* GOF mutations are associated with CID without endocrine or ectodermal manifestations.
- As most autosomal-dominant primary immunodeficiencies, *NFKB2* GOF changes have incomplete penetrance and variable expressivity.

NF-κB signaling through its *NFKB1*-dependent canonical and *NFKB2*-dependent noncanonical pathways plays distinctive roles in a diverse range of immune processes. Recently, mutations in these 2 genes have been associated with common variable immunodeficiency (CVID). While studying patients with genetically uncharacterized primary immunodeficiencies, we detected 2 novel nonsense gain-of-function (GOF) *NFKB2* mutations (E418X and R635X) in 3 patients from 2 families, and a novel missense change (S866R) in another patient. Their immunophenotype was assessed by flow cytometry and protein expression; activation of canonical and noncanonical pathways was examined in peripheral blood mononuclear cells and transfected HEK293T cells through immunoblotting, immunohistochemistry, luciferase activity, real-time polymerase chain reaction, and multiplex assays. The S866R change disrupted a C-terminal NF-κB2 critical site affecting protein phosphorylation and nuclear translocation, resulting in CVID with adrenocorticotropic hormone deficiency, growth hormone deficiency, and mild ectodermal dysplasia as previously described. In contrast, the nonsense mutations E418X and R635X observed in 3 patients led to constitutive nuclear localization and activation of both canonical and noncanonical NF-κB pathways, resulting in a combined immunodeficiency (CID) without endocrine or ectodermal manifestations. These changes were also found in 2 asymptomatic relatives. Thus, these novel *NFKB2* GOF mutations produce a nonfully penetrant CID phenotype through a different pathophysiologic mechanism than previously described for mutations in *NFKB2*. (*Blood*. 2017;130(13):1553-1564)

Introduction

Common variable immunodeficiency (CVID) is the most common symptomatic primary immunodeficiency (PID). Monogenic forms of CVID are thought to account for up to 10% of such patients; however, the recent cumulative discovery of >20 genes associated with CVID phenotypes, including *NFKB1* and *NFKB2*, is likely to result in an increased frequency of genetically defined patients with CVID.[1,2] Many of the recently described CVID-associated genes are inherited in an autosomal-dominant fashion and act either by haploinsufficiency, dominant-negative, or dominant gain-of-function (GOF) mechanisms. Incomplete immunologic or clinical penetrance, as well as variable clinical expressivity (more or less severe), have been described for several of these mutations.[2-6] As defined by International Union of Immunological Societies (IUIS) classification, "Combined immunodeficiencies generally less profound than severe combined immunodeficiency" encompasses a heterogeneous group of disorders with quantitative and/or functional T- and B-cell defects, including NF-κB signaling defects in *NIK* and *IKBKB* deficiency.[7] Some of the combined immunodeficiency defects can be difficult to discriminate from the more severe CVID cases.

The NF-κB signaling pathway has an important role in regulating lymphocyte development, immune responses, inflammation, cell proliferation, and cell death.[8-10] The NF-κB family is composed of 5 related transcription factors, including NF-κB1 p50/p105, NF-κB2 p52/p100, RelA, RelB, and c-Rel. These transcription factors share an N-terminal Rel homology domain (RHD) which also contains the dimerization, IκB-binding, and nuclear localization signals. RelA, RelB, and c-Rel contain a C-terminal transcriptional activation domain, which is absent in p50 and p52. Hence, p50 and p52 homodimers are transcriptionally repressive unless they are bound to RelA, RelB, or c-Rel. Two signaling pathways have been described to be associated with NF-κB: canonical and noncanonical. The canonical pathway utilizes NF-κB1, whereas the latter pathway involves NF-κB2. In a resting

Submitted 1 May 2017; accepted 9 July 2017. Prepublished online as *Blood* First Edition paper, 4 August 2017; DOI 10.1182/blood-2017-05-782177.

The online version of this article contains a data supplement.

The publication costs of this article were defrayed in part by page charge payment. Therefore, and solely to indicate this fact, this article is hereby marked "advertisement" in accordance with 18 USC section 1734.

state, NF-κB proteins are located in the cytoplasm and activation of either pathway is followed by phosphorylation, ubiquitination, and proteasomal processing of regulatory proteins allowing NF-κB1 and NF-κB2 to translocate to the nucleus and bind their specific gene targets. The canonical NF-κB pathway can be rapidly triggered by a variety of different stimuli, is independent of protein synthesis, and activates a spectrum of pro-inflammatory and anti-apoptotic genes. In contrast, noncanonical NF-κB activation is restricted to a number of agonists (eg, B-cell activating factor [BAFF], CD40L, lymphotoxin β, and receptor activator of NF-κB ligand [RANKL]), is slow and dependent on protein synthesis, and has a more limited but central role in cellular differentiation and development.[8-14] Germ line mutations in BAFF receptor gene *TNFRSF13C* have been associated with humoral immunodeficiency,[2] and somatic mutations activating the NF-κB2 pathway are described in hematologic malignancies,[15] both clinical features seen in patients with CVID.

Recently, germ line dominant-negative heterozygous *NFKB2* mutations were identified in patients diagnosed with early-onset CVID associated with autoimmunity, reduction in circulating B cells, adrenocorticotropic hormone (ACTH) insufficiency and occasional other pituitary hormone deficiencies, alopecia totalis or areata, and trachyonychia.[16-22] All reported mutations were confined to the C-terminal region of *NFKB2* leading to the disruption of p100 phosphorylation, inhibition of processing into the p52 active form, and prevention of nuclear translocation. This pathophysiologic mechanism is very similar to the one described in *Nfkb2* Lym1-mutated mice containing p.Y868X mutations encoding a nonprocessable form of p100.[23] These mice also have phenotypes that are similar to those seen in $NIK^{-/-}$ or alymphoplasia (aly) mutant mice, severely defective in p52 generation, impaired B-cell maturation, and lymphoid organogenesis.[24,25]

In our study, while evaluating 4 genetically uncharacterized PID patients from 3 unrelated families, we found 3 new heterozygous *NFKB2* mutations. Mutation S866R was detected in a patient with CVID, endocrinopathy, and mild ectodermal dysplasia, and acting mechanistically similar to previously reported mutations in this gene. This contrasts with 3 patients from 2 families who presented with CID without endocrine or ectodermal manifestations and carrying mutations E418X and R635X that resulted in constitutive NF-κB2 activation, nuclear localization, and gene transcription. These patients demonstrate that GOF mutations in *NFKB2* acting through this immunopathologic mechanism are associated with a distinctive and complex immune disorder. Two asymptomatic relatives of the patients carrying the same *NFKB2* GOF mutations were also identified.

Materials and methods

Next-generation sequencing: targeted next-generation sequencing and whole-exome sequencing

For targeted next-generation sequencing in family A, capture of the target regions, including the coding exons plus 50 flanking bases of 320 genes was performed with reagents from a custom-designed HaloPlex Target Enrichment kit (Agilent Technologies), according to the HaloPlex Target Enrichment System Protocol. Capture of the target regions, including the coding exons plus 50 flanking bases of 320 genes was performed with reagents from a custom-designed HaloPlex Target Enrichment kit (Agilent Technologies), according to the HaloPlex Target Enrichment System Protocol. Briefly, the protocol consisted of the following steps: (1) digestion of genomic DNA (gDNA) with restriction enzymes; (2) hybridization of fragments to probes whose ends are complementary to the target fragments (during this step, fragments are circularized and sequencing and barcode adapters are incorporated); (3) capture of target DNA using streptavidin beads and ligation of circularized fragments; and (4) polymerase chain reaction (PCR) amplification of captured target libraries. Quality control of all libraries was performed on the Agilent Bioanalyzer using a high-sensitivity chip. Template dilutions were calculated after library concentrations were normalized to ~100 pM using the Ion Library Equalizer kit (Life Technologies). Library templates were clonally amplified and enriched using the Ion Chef (Life Technologies) according to the manufacturer's protocol. Samples were subjected to the standard Ion Proton PI chip v3 (Life Technologies).

Whole-exome sequencing (WES) was performed using the Ion Torrent AmpliSeq RDY Exome kit (Life Technologies) and the Ion Chef and Proton instruments (Life Technologies) in family B. Briefly, 100 ng of gDNA was used as the starting material for the AmpliSeq RDY Exome amplification step following the manufacturer's protocol. Library templates were clonally amplified and enriched using the Ion Chef and the Ion PI Hi-Q Chef kit (Chef package version IC.4.4.2; Life Technologies), following the manufacturer's protocol. Enriched, templated Ion Sphere Particles were sequenced on the Ion Proton sequencer using the Ion PI chip v3 (Life Technologies). For family C, the ACE Clinical Exome Test (Personalis Inc) was also used. Briefly, sequence alignment and variant calling were performed using Personalis ACE pipeline analysis. Variants were annotated and filtered using Ingenuity (Qiagen).

Bioinformatics analysis

Read mapping and variant calling were performed using Ion Torrent Suite software v4.4.2. In short, sequencing reads were mapped against the University of California, Santa Cruz (UCSC) hg19 reference genome using the Torrent Mapping Alignment Program (TMAP) map4 algorithm. Single-nucleotide polymorphisms (SNPs) and insertions/deletions (INDELS) were called by the Torrent Variant Caller plugin (v.4.414-1) using the "Generic-Proton-Germ Line: Low Stringency" configuration. Only reads that were unambiguously mapped were used for variant calling. Variants were annotated using ANNOVAR (http://annovar.openbioinformatics.org/). Data mining, biological interpretation, and candidate gene discovery were performed using various online tools including The Database for Annotation, Visualization and Integrated Discovery (DAVID; https://david.ncifcrf.gov), and GeneCards (http://www.genecards.org). Target coverage was evaluated using the Torrent Coverage Analysis plugin (v.4.414-1), and the output was further evaluated using in-house, custom Perl scripts.

Sanger sequencing

NFKB2 Sanger sequencing was performed to confirm WES-detected variants and to screen family members. gDNA was PCR-amplified using GoTaq polymerase (Promega) and exon-specific primers. Amplicons were bidirectly sequenced using the Big Dye Terminator version 1.1 cycle sequencing kit and an Applied Biosystems 3130xl Genetic Analyzer (Life Technologies).

Cell culture

Peripheral blood mononuclear cells (PBMCs) were isolated by the use of Ficoll-Paque Plus (GE Healthcare). PBMCs were cultured in RPMI 1640 with 10% fetal bovine serum, 2 mM L-glutamine, 100 U/mL penicillin, and 100 μg/mL streptomycin (Thermo Fisher Scientific) at 37°C in a humidified 5% CO_2 incubator. HEK293T cells were cultured in Dulbecco modified Eagle medium with10% fetal bovine serum.

Plasmid preparation

Human NF-κB2 (*NFKB2*) and NF-κB–inducing kinase (NIK) (*MAP3K14*) DNA were purchased (Dharmacon) and subcloned into the mammalian expression vector pcDNA3-HA or pFlag-CMV2. Indicated mutants for the *NFKB2* were generated based on the site-directed mutagenesis protocol using AccuPrime Pfx DNA Polymerase, followed by *Dpn*I treatment (Thermo Fisher Scientific).

Immunoprecipitation and western blots

Expression vectors (pcDNA3-HA-*NFKB2* wild type [WT] or mutant with or without pFlag-CMV2-NIK) were transfected into HEK-293T cells using Effectine transfection reagent (Qiagen). Nuclear and cytosolic extracts were obtained with NE-PER nuclear and cytoplasmic extraction reagent (Thermo Scientific), sequentially incubated with mouse anti-hemagglutinin (HA) antibody (Covance)

and protein A/G-agarose beads (Pierce). Beads were washed, resuspended, boiled, and separated on NuPAGE Novex 4% to 12% Bis-Tris protein gels. Subsequent western blot analysis was performed with the mouse anti-HA monoclonal antibody (Covance), NIK (Cell Signaling Technology), RelB (Santa Cruz Biotechnology). Glyceraldehyde-3-phosphate dehydrogenase (GAPDH) and Lamin A/C antibodies (Cell Signaling Technology) were used as controls for the purity of the cytoplasmic and nuclear fractions, respectively.

For NF-κB2 expression from patient's cells, total PBMCs were stimulated with anti-CD3 (OKT3, 1 μg/mL; eBioscience) for 48 hours. Cell lysates were prepared and analyzed with anti-phospho-NF-κB2 (S866/S870) and anti-NF-κB2 (Cell Signaling Technology). Immunoblotting of β-actin was used as a loading control.

Fluorescence microscopy

HEK-293T cells were seeded in 24-well plates and transfected with the indicated plasmid using Effectene (Qiagen). The cells were sequentially washed, fixed, and permeabilized before incubation with blocking buffer and mouse anti-HA monoclonal antibody (Covance), and/or rabbit anti-Flag polyclonal affinity antibody (Sigma). The cells were then washed and incubated with either Alexa Fluor 488 (green color) or Alexa Fluor 568 (red color)–conjugated secondary antibodies in blocking buffer. Images were collected using a ZOE fluorescent cell imager (Bio-Rad).

Gene expression

Total RNA was isolated from PBMCs with the RNeasy Plus mini kit (Qiagen) and reverse transcribed by use of the iScript complementary DNA (cDNA) synthesis kit (Bio-Rad). Gene expression was analyzed by real-time PCR using a TaqMan probe (CXCL13 and 18S ribosomal RNA [rRNA]; Applied Biosystems) and StepOne Plus real-time PCR (Applied Biosystems) according to the manufacturer's instructions. All reactions were performed in triplicate for 40 cycles. 18S rRNA was used as the endogenous control, and gene expression of *CXCL13* was quantitatively measured relative to healthy donors or control samples. The relative quantification of *CXCL13* expression was calculated with the comparative Ct method. For each sample, the threshold cycle (Ct) was determined, and the relative fold expression was calculated as follows: ΔCt = Ct of target gene − Ct of 18S rRNA. For *CXCL13* gene expression in T-cell receptor (TCR)-stimulated samples from healthy donor controls or patients: $\Delta\Delta Ct = \Delta Ct$ of each sample − ΔCt of healthy donor control; for small interfering RNA (siRNA) experiment: $\Delta\Delta Ct = \Delta Ct$ of each sample − ΔCt of control siRNA sample; for overexpression of WT or mutant in total PBMCs: $\Delta\Delta Ct = \Delta Ct$ of each sample − ΔCt of WT. The relative fold expression was calculated using the equation $2^{-\Delta\Delta Ct}$.

Luciferase assay

HEK-293T cells growing in 24-well plates were cotransfected with pGL4.32-NF-κB and indicated pcDNA3-HA-NFKB2 expression vector. The next day, cells were treated with tumor necrosis factor α (TNFα; 100 ng/mL) for 5 hours and luciferase activities were measured using the luciferase assay kit (Promega).

Statistical analysis

When indicated, data were analyzed using GraphPad Prism software. The differences were considered significant when $P < .05$.

All participants underwent the informed consent process and enrolled on an institutional review board–approved National Institute of Allergy and Infectious Diseases, National Institutes of Health research protocol. This study was conducted in accordance with the Declaration of Helsinki.

Results

Clinical summaries

Patient A1 is a 30-year-old Caucasian man who first showed evidence of a compromised immune function during infancy with severe, recurrent pneumonias requiring several hospitalizations and immunoglobulin G (IgG) replacement therapy. At 21 years of age, he was diagnosed with primary sclerosing cholangitis. Splenomegaly, thrombocytopenia, and intermittent lymphadenopathy were also part of his clinical manifestations. His immune phenotype was characterized by hypogammaglobulinemia (IgG, 1.95 g/L; IgA and IgM, undetectable), panlymphopenia (absolute lymphocyte count 0.308×10^9/L; $CD3^+$, 0.25×10^9/L, $CD19^+$, 0.02×10^9/L; $CD16/56^+$, 0.02×10^9/L) and decreased lymphocyte proliferative responses to mitogens. His family history is significant for his father who was asymptomatic until the age of 48 years at which time he was diagnosed with rheumatoid arthritis (A2).

Patient B1 is a 33-year-old Caucasian woman who was healthy until the age of 14 years when she presented with a severe Epstein-Barr virus (EBV) infection and massive splenomegaly that ultimately required splenectomy. At 19 years of age, she first developed respiratory symptoms. In subsequent years, caseating granulomas, cytomegalovirus (CMV) pneumonitis, and granulomatous lymphocytic interstitial pneumonitis with bronchiolitis obliterans were diagnosed. T-cell large granular lymphocytic leukemia with pure red blood cell aplasia, CMV enteritis, warts, mucocutaneous candidiasis, and splenomegaly were also part of her clinical manifestations. Her immunophenotype is characterized by hypogammaglobulinemia (IgG, 3.18 g/L; IgA, <0.01 g/L; IgM, 0.31 g/L) with B-cell lymphopenia ($CD19^+$, 0.018×10^9/L), and T-cell lymphocytosis ($CD3^+$ 5.845×10^9/L) with poor T-cell proliferation to mitogens and antigens. Her family history is significant for 1 symptomatic brother (B2, see next paragraph) and 1 asymptomatic brother (B3).

Patient B2 is the 28-year-old younger brother of B1 who has a history of recurrent upper and lower respiratory infections starting in infancy; he was diagnosed with CVID at 12 years of age at which time IVIG replacement was initiated. During adulthood, he developed *Pneumocystis jirovecii* pneumonitis, mucocutaneous candidiasis, warts, chronic noninfectious diarrhea, and splenomegaly. His immunophenotype is characterized by hypogammaglobulinemia (IgG, 2.65 g/L; IgA, <0.02 g/L; IgM, 0.24 g/L) with B-cell lymphopenia ($CD19^+$, 0.02×10^9/L), and T-cell lymphocytosis ($CD3^+$, 2.284×10^9/L) with normal T-cell proliferations to mitogens and antigens.

Patient C1 is a 14-year-old Caucasian boy with an unremarkable infection history. He was diagnosed with ACTH deficiency at 8 years of age, and growth hormone (GH) deficiency at age 10. His immunophenotype is characterized by hypogammaglobulinemia (IgG, 2.41 g/L; IgA, 0.1 g/L; IgM, 0.23 g/L) with normal B-cell numbers ($CD19^+$, 0.298×10^9/L) and vaccine responses, and T-cell lymphocytosis ($CD3^+$, 4.494×10^9/L) with normal T-cell proliferation to mitogens and antigens (for aggregated clinical and laboratory data, see Table 1 and supplemental Clinical Summaries [available on the *Blood* Web site]).

Exome sequencing and genetic analysis

Heterozygous *NFKB2* mutations (*NFKB2* NM_001077494 c.1252G>T, p.E418X; c.1903C>T, p.R635X; and c.2596A>C, p.S866R) were detected by next-generation sequencing. Briefly, the nonsense variant *NFKB2* c.1252G>T, p.E418X was detected by targeted next-generation sequencing and is not reported in the ExAC or 1000G databases, and was predicted to result in nonsense-mediated decay (NMD) as it creates a premature termination codon that precedes an exon-exon junction by >50 to 55 nucleotides. It was strongly predicted to be deleterious by CADD (Combined Annotation Dependent Depletion) (phred = 34) and DANN (Deleterious Annotation of genetic variants using Neural Networks) (0.984). This variant was confirmed by Sanger sequencing and

Table 1. Clinical and laboratory features in patients with heterozygous *NFKB2* mutations

ID *NFKB2* mutation	A1 (p.E418X)	A2 (p.E418X)	B1 (p.R635X)	B2 (p.R635X)	B3* (p.R635X)	C1 (p.S866R)
Age, y/sex	28/M	63/M	33/F	28/M	20/M	14/M
Abs no. of lymphocytes, $\times 10^9$/L	**0.308**	1.05	*6.14*	*2.371*	n.a	*4.96*
$CD3^+$, abs no., $\times 10^9$/L (%)	**0.25** (*82*)	0.822 (78)	*5.845 (95)*	*2.284 (96)*	**(36)**	*4.494 (90.6)*
$CD4^+/CD3^+$, $\times 10^9$/L (%)	**0.17** (58)	0.684 (*65*)	0.792 (**12.9**)	**0.423 (18)**	**7.3**	*2.981* (60.1)
$CD62L^+/CD45RA^+$, $\times 10^9$/L (%)	**0.043** (12.7)	0.189 (18)	0.172 (**2.8**)	n.a	n.a	*2.252 (45.4)*
$CD62L^+/CD45RA^-$, $\times 10^9$/L (%)	**0.14** (*41.1*)	0.376 (*35.8*)	0.381 (**6.2**)	n.a	n.a	0.397 (**8**)
$CD62L^-/CD45RA^-$, $\times 10^9$/L (%)	**0.03** (8.7)	0.117 (11.1)	*0.233* (3.8)	n.a	n.a	0.084 (**1.7**)
$CD62L^-/CD45RA^+$, $\times 10^9$/L (%)	0 (0)	0.002 (0.2)	0.006 (0.1)	n.a	n.a	*0.248 (5)*
$CD8^+/CD3^+$, $\times 10^9$/L (%)	0.07 (23.6)	**0.105 (10)**	*4.937 (80.4)*	*1.843 (77.7)*	**(12.8)**	*1.235* (24.9)
$CD62L^+/CD45RA^+$, $\times 10^9$/L (%)	**0.052** (15.2)	**0.044 (4.2)**	*1.345 (21.9)*	n.a	n.a	*0.957* (19.3)
$CD62L^+/CD45RA^-$, $\times 10^9$/L (%)	**0.019** (5.5)	**0.024** (2.3)	*0.141* (2.3)	n.a	n.a	**0.02 (0.4)**
$CD62L^-/CD45RA^-$, $\times 10^9$/L (%)	**0.008** (2.3)	**0.027** (2.6)	*0.393* (6.4)	n.a	n.a	0.04 (**0.8**)
$CD62L^-/CD45RA^+$, $\times 10^9$/L (%)	**0.003** (0.9)	**0.011** (1)	*3.058 (49.8)*	n.a	n.a	*0.218* (4.4)
$CD19^+$, abs no., $\times 10^9$/L (%)	**0.02** (6)	0.154 (14.7)	**0.018 (0.3)**	**0.02 (0.8)**	*(33.7)*	0.308 (6.2)
$CD19^+/CD38^+$: $\times 10^9$/L (%)	**0.02** (6)	0.143 (13.6)	n.a	n.a	n.a	0.298 (6)
$CD19^+/CD27^+/IgM^+$, $\times 10^9$/L (%)	**0 (0)**	**0.005** (0.5)	n.a	n.a	n.a	**0 (0)**
$CD19^+/CD27^+/IgM^-$, $\times 10^9$/L (%)	**0 (0)**	**0.001 (0.1)**	n.a	n.a	n.a	**0.005 (0.1)**
NK cells, abs no., $\times 10^9$/L (%)	**0.02** (6.5)	**0.075** (7.1)	0.258 (4.2)	**0.064 (2.7)**	*(30)*	0.188 (3.8)
$CD3^+/CD4^+/RA^+/CD31^+$,* %	5.9	4.4	**1.5**	1.9	1.9	37.7
$CD3^+/CD4^+/RA^-/CXCR5^+$,* %	4.2	**0.3**	**0.1**	**0.5**	**0.5**	**0.5**
$CD4^+/CD3^+$ Vβ spectratyping*	Normal distribution	Normal distribution	Normal distribution	Normal distribution	Normal distribution	Normal distribution
$CD8^+/CD3^+$ Vβ spectratyping*	Normal distribution	Normal distribution	*Vβ 22 expansion in CD8 cells*	Normal distribution	Normal distribution	Normal distribution
Lymphocyte proliferations†						
Mitogens and antigens	PHA <20% ConA <20% PWM <20% Tetanus <1% Candida <1%	n.a	PHA <50% ConA <50% PWM normal Tetanus normal	PHA normal ConA normal PWM normal Tetanus normal	n.a	PHA normal ConA normal PWM normal
Immunoglobulins, g/L						
IgG	1.95‡,§	n.a	14.44‡	**2.65**	n.a	**2.41**
IgA	**<0.01**	n.a	**<0.01**	**<0.02**	n.a	**0.1**
IgM	**<0.01**	n.a	**0.22**	**0.24**	n.a	**0.23**

Numbers/terms in italics/bold indicate values above/below the normal range, respectively, compared with age-matched controls.

Abs no., absolute number; ACTH, adrenocorticotropic hormone; CMV, cytomegalovirus; ConA, concanavalin A; EBV, Epstein-Barr virus; F, female; GH, growth hormone; HiB, *H influenzae* B; HPV, human papillomavirus; ID, identification; M, male; n.a, data not available; NK, natural killer; PBMC, peripheral blood mononuclear cell; PHA, phytohemagglutinin; Pj, *P jirovecii*; PWM, pokeweed mitogen; s/p, status post; T-LGL, T-cell large granular lymphocyte.

*Tested on frozen PBMCs.

†In percentage values when compared with the healthy control normal ranges at the center the study was performed.

‡On IgG replacement therapy.

§Partial adherence to therapy.

Table 1. (continued)

ID *NFKB2* mutation	A1 (p.E418X)	A2 (p.E418X)	B1 (p.R635X)	B2 (p.R635X)	B3* (p.R635X)	C1 (p.S866R)
Vaccine responses						
	Not tested; on IgG replacement	Not tested	Poor response to pneumococcal polysaccharide vaccination	Not tested	Not tested	Protective titers to hepatitis A, tetanus and diphteria toxoids, HiB, and pneumococcal polysaccharide vaccination
Clinical history						
	Recurrent sinusitis and pneumonias; splenomegaly; thrombocytopenia; lymphadenopathy; lymphopenia; primary sclerosing cholangitis	Asymptomatic until the age of 48 y; rheumatoid arthritis	T-LGL leukemia (with red cell aplasia); T-cell lymphocytosis; lymphocytic interstitial pneumonitis; bronchiolitis obliterans; bronchiectasis; onychomycosis; esophageal candidiasis; warts; recurrent herpes labialis; HPV cervical intraepithelial neoplasia; EBV viremia; CMV viremia; chronic diarrhea; splenomegaly (s/p splenectomy); basal cell carcinomas	Recurrent sinusitis, otitis, and pneumonias; Pj pneumonia; bronchiectasis; recurrent thrush; warts; mild microcytic anemia; mild thrombocytopenia; splenomegaly; chronic diarrhea (not infectious)	Asymptomatic	Spontaneously controlled molluscum contagiosum; ACTH deficiency; GH deficiency

Numbers/terms in italics/bold indicate values above/below the normal range, respectively, compared with age-matched controls.

Abs no., absolute number; ACTH, adrenocorticotropic hormone; CMV, cytomegalovirus; ConA, concanavalin A; EBV, Epstein-Barr virus; F, female; GH, growth hormone; HiB, *H influenzae* B; HPV, human papillomavirus; ID, identification; M, male; n.a, data not available; NK, natural killer; PBMC, peripheral blood mononuclear cell; PHA, phytohemagglutinin; Pj, *P jirovecii*; PWM, pokeweed mitogen; s/p, status post; T-LGL, T-cell large granular lymphocyte.

*Tested on frozen PBMCs.

†In percentage values when compared with the healthy control normal ranges at the center the study was performed.

‡On IgG replacement therapy.

§Partial adherence to therapy.

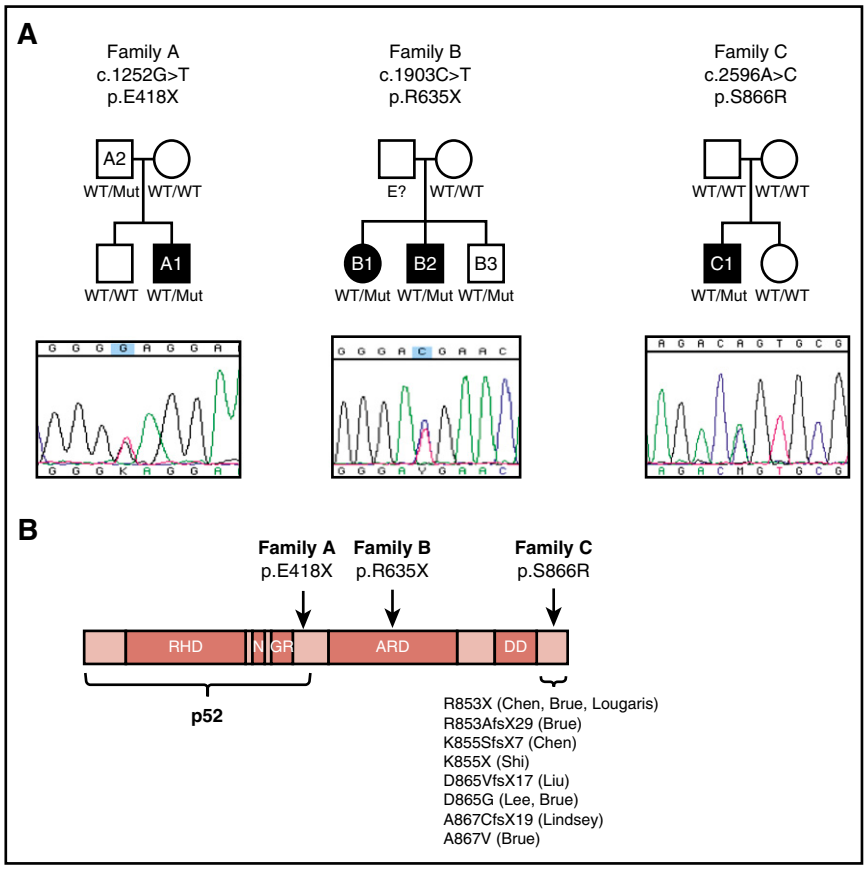

Figure 1. Genetics and pedigrees of families with *NFKB2* mutations. (A) Pedigrees and Sanger sequencing of families with *NFKB2* mutations. Mutation status of *NFKB2* c.1252G>T for family A, *NFKB2* c.1903C>T for family B, and *NFKB2* c.2596A>C for family C are indicated for each individual. Pedigree with those affected shown in black filled symbols. (B) Schematic of NF-κB2 with the Rel homology domain (RHD), nuclear localization signal (N), glycin-rich region (GR), ankyrin repeat domain (ARD), and death domain (DD). The amino acid sequence and location for affected individuals are shown with arrow.

was also identified in the proband's unaffected father (Figure 1). The *NFKB2* c.1903C>T, p.R635X variant was detected by WES. One heterozygous occurrence of the *NFKB2* c.1903C>T, p.R635X variant is reported in the ExAC database (rs748910652, T = 1.022e-05, 1/97872); no homozygotes are reported. This nonsense variant was predicted to result in NMD, and was strongly predicted to be deleterious by CADD (phred = 38) and DANN (0.994). The nucleotide position and region are conserved (GERP^{++} [Genetic Evolutionary Rate Profiling] = 4.43, SiPhy [SIte-specific PHYlogenetic analysis] = 11.698). This variant was confirmed by Sanger sequencing and also identified in the proband's unaffected brother. The missense variant *NFKB2* c.2596A>C, p.S866R was detected by WES in the proband and not in his parents or sibling. This variant is not reported in the ExAC or 1000G databases, and was predicted to abrogate MAP3K14-induced phosphorylation at serine 866.

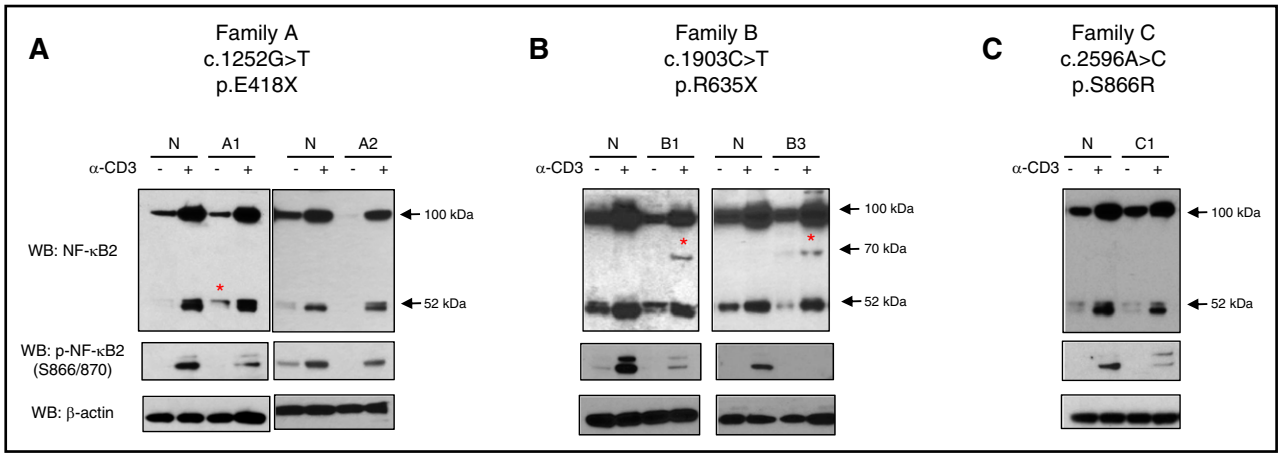

Figure 2. NF-κB2 protein expression in PBMCs. (A-C) Immunoblot of wild-type and mutant NF-κB2 in PBMCs from healthy normal control and patients. Total PBMCs were treated with α-CD3 to stimulated NF-κB2 pathway for 48 hours. Cell lysates were prepared and analyzed for phosphorylation of p100 and for full-length (p100) and active form (p52), and mutant expression by western blotting. Immunoblotting of β-actin was used as a loading control. Red asterisks indicate mutant form of NF-κB2 in patient cells. Due to the similar size between mutant E418X and active form of NF-κB2 (p52), it was difficult to discriminated mutant (E418X) from active form of NF-κB2 in stimulated condition in patient A1.

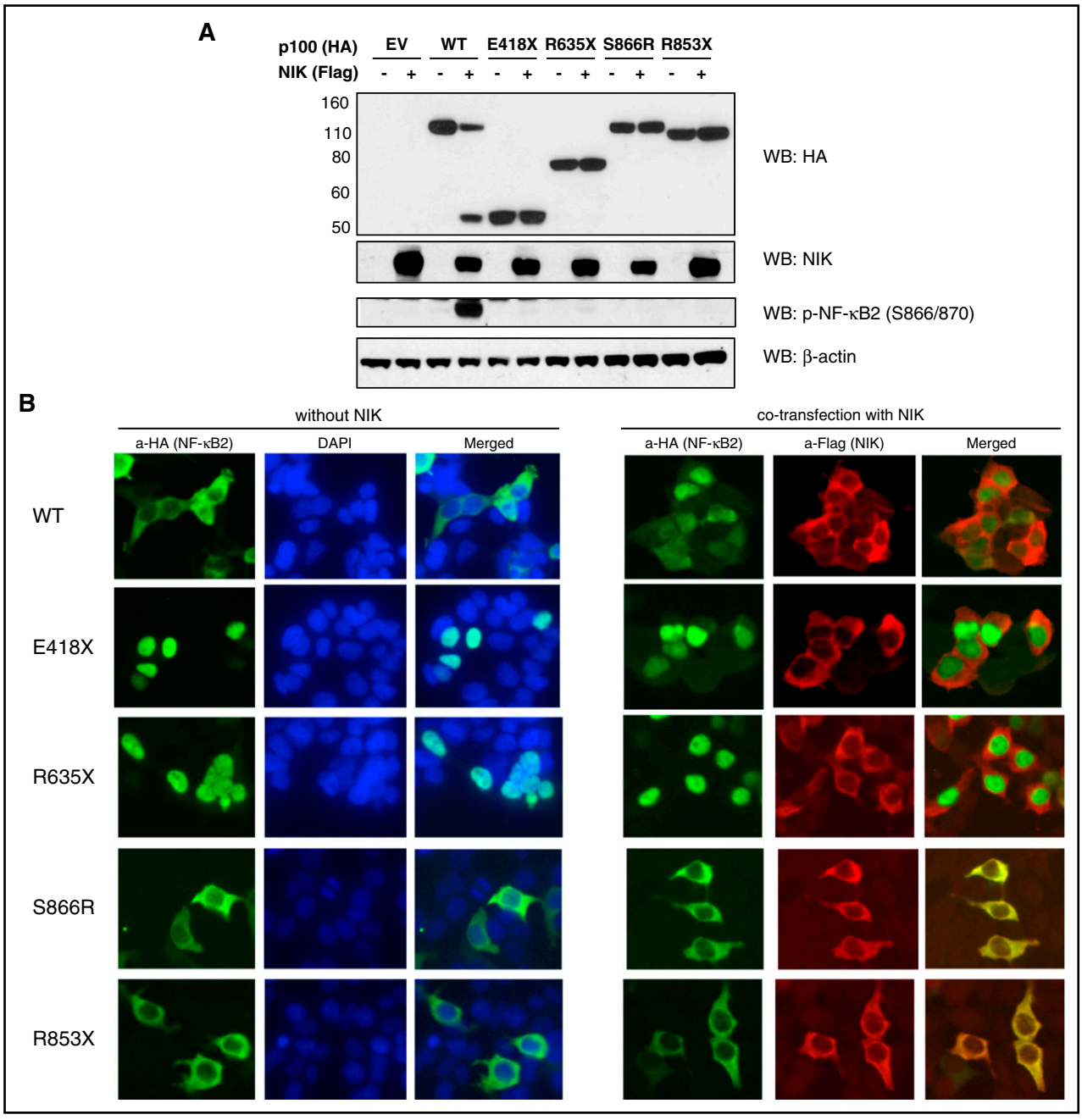

Figure 3. Protein expression and localization of mutant NF-κB2 in transfected cells. (A) HEK293T cells were transiently transfected with the indicated constructs in the presence and absence of NIK coexpression. Cell lysates were analyzed for phosphorylation of p100 and for p100, p52, and mutant expression by western blotting. E418X mutant size was closed to the active form p52. All other mutants are failed phosphorylation and processing to p52 in the presence of NIK expression. Molecular weight markers are indicated on the left size (kilodaltons). (B) HEK293T cells were transiently transfected indicated WT or mutant vector (pcDNA3-HA) with or without Flag-NIK. Nucleus was labeled with DAPI (blue). Original magnification ×175. Cells were stained with anti-Flag and anti-HA antibody, followed by Alexa 488-conjugated (for HA-NF-kB2, green) and Alexa 568-conjugated (for Flag-NIK, red) secondary antibody. Data shown are representative of 3 experiments.

Mutant NF-κB2 protein expression in PBMCs

Whole-cell lysates from PBMCs were tested for NF-κB2 expression. The noncanonical signaling pathway has been well described in B cells and stromal cells, and known to be activated by a limited set of agonists including lymphotoxin, RANKL, CD40L, and BAFF.[14] However, due to the low number of B cells in patients A1 and B1 (cells from B2 were not available for the study), we tested NF-κB2 expression in TCR-stimulated-PBMCs which are also known to activate this pathway in a later stage of an immune response.[26] Although NMD was predicted, immunoblotting confirmed the expression of the mutant form of NF-κB2, E418X (~50 kDa) and R635X (~70 kDa) (Figure 2). Patients' cells showed decreased phosphorylation of p100 and processed form (p52) following activation. Cells from asymptomatic relatives A2 and B3 also showed reduced p100 phosphorylation and processed p52, but mutant protein expression was not detected in A2. The fourth patient had a heterozygous missense mutation in serine 866, a critical phosphorylation site for ubiquitination and proteasomal

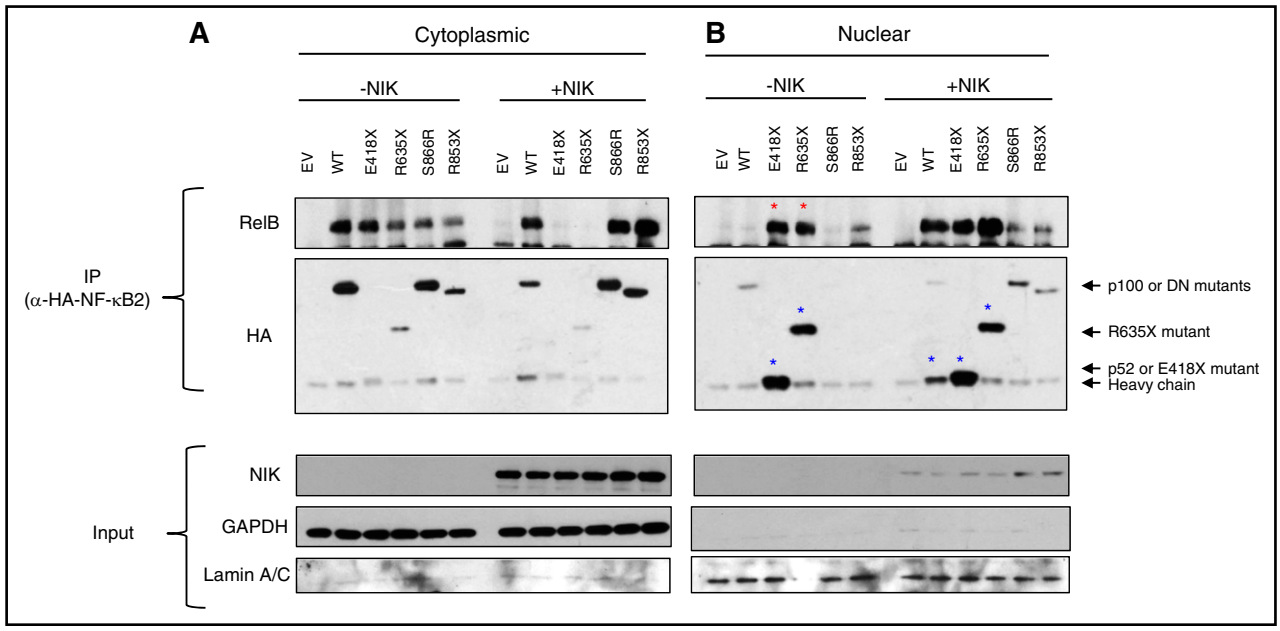

Figure 4. Increased interaction of RelB with mutant E418X, R635X in nuclear fraction. HEK293T cells were transiently transfected with the indicated constructs in the presence and absence of NIK coexpression. (A) Cytoplasmic and (B) nuclear fractions were prepared, and immunoprecipitated with an α-HA antibody. Cell lysates from IP samples were analyzed for the interaction of NF-κB2 (WT or mutants) with RelB. The faint band at 50 kDa in all lanes is immunoglobulin heavy chain. Immunoblotting of Lamin A/C and GAPDH was used as a marker for the nuclear and cytoplasmic fraction, respectively. Red asterisks indicate increased interaction of mutant E418X, R635X with RelB without NIK expression. Blue asterisks indicate increased translocation of mutant forms E418X, R635X, and active form of NF-κB2 (p52) to the nucleus. Data shown are representative of 3 experiments.

processing of p100 to generate p52. As expected, reduced phosphorylation of NF-κB2 and expression of p52 were detected in patient C1 (Figure 2).

Increased nuclear translocation of mutants NFKB2 and RelB

NF-κB2 mutant constructs were tested for protein expression and function. Human embryonic kidney (HEK) 293T-cell were transiently transfected with the mutant constructs as well as with a construct from the previously reported dominant-negative mutant (R853X). Noncanonical NF-κB signaling depends on NIK (*MAP3K14*) accumulation, which becomes stabilized by TNF superfamily signaling.[27] To mimic the activation status of the noncanonical signaling pathway, we cotransfected NIK together with vectors expressing either the WT or mutant *NFKB2* alleles. Western blots showed that WT-p100 protein was processed to the active form p52 upon cotransfection of NIK, whereas the mutants R635X, S866R, and R853X failed to produce phosphorylation preventing subsequent proteasomal processing into active p52 (Figure 3A). Although results with the mutant E418X were less categorical in terms of p52 processing as the predicted molecular weight of the mutated protein overlaps that of processed p52, this mutant failed to undergo phosphorylation. It has been previously established that 2 serine sites (S866 and S870) in the C terminus of p100 are required for NIK-induced processing to p52 that translocates to the nucleus.[14] Therefore, we tested protein localization in the absence or presence of NIK. As shown in Fig 3B, WT NF-κB2 was found mostly in the cytoplasm, whereas cotransfection of WT with NIK induced p52 nuclear translocation. Although C terminus mutants S866R and R853X failed nuclear translocation upon NIK vector cotransfection, mutants E418X and R635X were readily detected exclusively in the nucleus in the absence or presence of NIK expression. These results demonstrated that the mutants E418X and R635X escape cytoplasmic retention and behave like activated p52.

Under resting conditions, a p100:RelB heterodimer remains sequestered in the cytoplasm as a result of the C-terminal IκB-like inhibitory domain of p100.[28] Activation of the noncanonical signaling increases processing of p100 to p52, enabling the heterodimer p52:RelB to translocate into the nucleus, where it regulates activation of transcription. Therefore, we investigated whether nuclear-translocated NF-κB2 mutants altered RelB localization. Without NIK expression, the majority of RelB is localized in the cytoplasmic fraction. However, coexpression of WT NF-κB2 and NIK induced processing of p100 to active p52 and increased translocation of RelB into the nucleus (Figure 4). Consistent with our immunohistochemistry findings, the mutants E418X and R635X were primarily detected in the nuclear fraction. Increased nuclear translocation was also detected when patient's B1(R635X) PBMCs were tested (not shown). Also, overexpression of these mutants increased interaction with RelB and translocation to the nucleus in the absence of NIK expression, whereas the dominant-negative mutants R853X and S866R resulted in retention of RelB in the cytoplasm even in the presence of NIK (Figure 4). These results demonstrate distinctly different activity for the mutations E418X and R635X compared with the previously reported dominant-negative mutations.

To test for levels of noncanonical NF-κB activation upon NF-κB2:RelB heterodimer nuclear translocation, we used reverse transcription–PCR to assay *CXCL13*, a known noncanonical NF-κB target gene.[26] In TCR-stimulated PBMCs, knockdown of *NFKB2* decreased *CXCL13* gene expression (Figure 5A), whereas overexpression of E418X and R635X increased *CXCL13* transcription when compared with the cells transfected with WT (Figure 5B). Consistent with the result from the transfected cells, patient B1's $CD4^+$ T cells showed a 20-fold increase in *CXCL13* gene transcription compared with healthy controls (Figure 5C), suggesting that activated forms of mutant NF-κB2 (ie, E418X and R635X) but not a dominant-negative form (ie, S866R) increase noncanonical NF-κB signaling and induce target gene

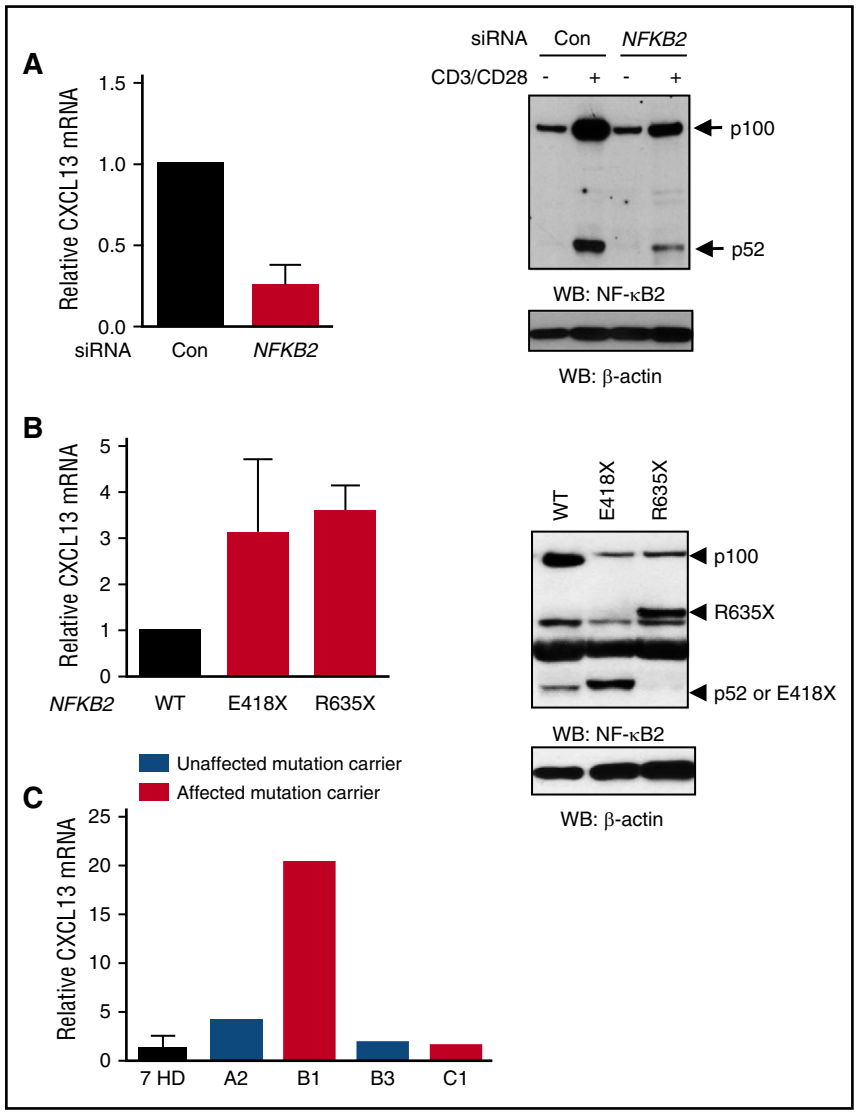

Figure 5. Regulation of CXCL13 gene expression by NF-κB2 protein. (A-B) Indicated siRNA or pcDNA3-HA-*NFKB2* (WT or mutants) were transfected into total PBMCs from healthy donor control. Next day, cells were washed and stimulated with Dynabeads-CD3/28 for 48 hours. RNA was prepared and *CXCL13* gene expression was analyzed by real-time PCR. A fold change was calculated for *NFKB2* siRNA or mutants with control vector (A) or WT (B) transfected cells, normalize to 1. *CXCL13* was not detected in unstimulated samples. Decreased NF-κB2 (A) or overexpressed WT or mutant protein expression (B) was confirmed by western blot. Results shown are means + standard error of the mean of 3 independent experiments. (C) CD4 T cells were enriched using stem cell negative selection kit and cells were stimulated with Dynabeads-CD3/28 for 48 hours. Levels of *CXCL13* mRNA in activated CD4 T cells from indicated patients were measured by real-time PCR using the probe for *CXCL13* and normalized to 18S rRNA. *CXCL13* expression was not detected in A1 due to low cell number. Data are means value of replicates from indicated patients. For relative gene expression, all data were normalized to the paired normal control.

activation. Cells from asymptomatic relatives A2 and B3 showed *CXCL13* transcription levels similar to healthy controls.

Cross-talk between noncanonical and canonical NF-κB pathway

It has been established that NF-κB2 p100 exhibits an IκB-like activity, which inhibits the canonical NF-κB pathway.[8,29] To examine whether different forms of the NF-κB mutants affect the canonical pathway, we tested NF-κB luciferase activity in HEK293T-transfected cells. TNF-α stimulation strongly increased NF-κB activity in the cells transfected with empty vector. Expression of WT or dominant-negative mutants S866R and R853X markedly inhibited NF-κB activity. In contrast, E418X and R635X mutants exerted a reduced inhibitory effect on TNF-α–induced canonical NF-κB pathway (Figure 6A). Moreover, lipopolysaccharide (LPS)-induced interleukin 6 (IL-6) and TNF-α production was increased about twofold in patient A1 and B1 but not in C1 (Figure 6B), suggesting that NF-κB2 mutants lacking its C-terminal IκB-like inhibitory domain, result in both overproduction of its p52 active form and disruption of its inhibitory IκB-like function.

Discussion

NF-κB canonical and noncanonical signaling pathways play critical roles in B-cell differentiation and function.[10,30] *Nfkb1* or *Nfkb2* knockout mice show defective B-cell maturation and impaired humoral immune response[31,32] and both *NFKB1* and *NFKB2* mutations have been identified in patients with CVID.[16-22,33] Germ line heterozygous dominant-negative *NFKB2* mutations in CVID patients that encode for C-terminal–mutated forms of nonprocessable p100 proteins preventing p52 formation, affecting NF-κB noncanonical signaling and resulting in antibody deficiency, lymphocyte dysfunction, central adrenal insufficiency, alopecia totalis or areata, and trachyonychia were recently identified.[16-22] Mutations in *RELB* (null, homozygous), also affecting NF-κB noncanonical signaling, have been identified in 3 patients from a single consanguineous family. Their phenotype was characterized as an early onset combined immunodeficiency presenting with failure to thrive, lung complications (chronic cough, infections, and pneumothorax), polyarthritis, ecthyma gangrenosum and mostly functional T- and B-cell defects.[34]

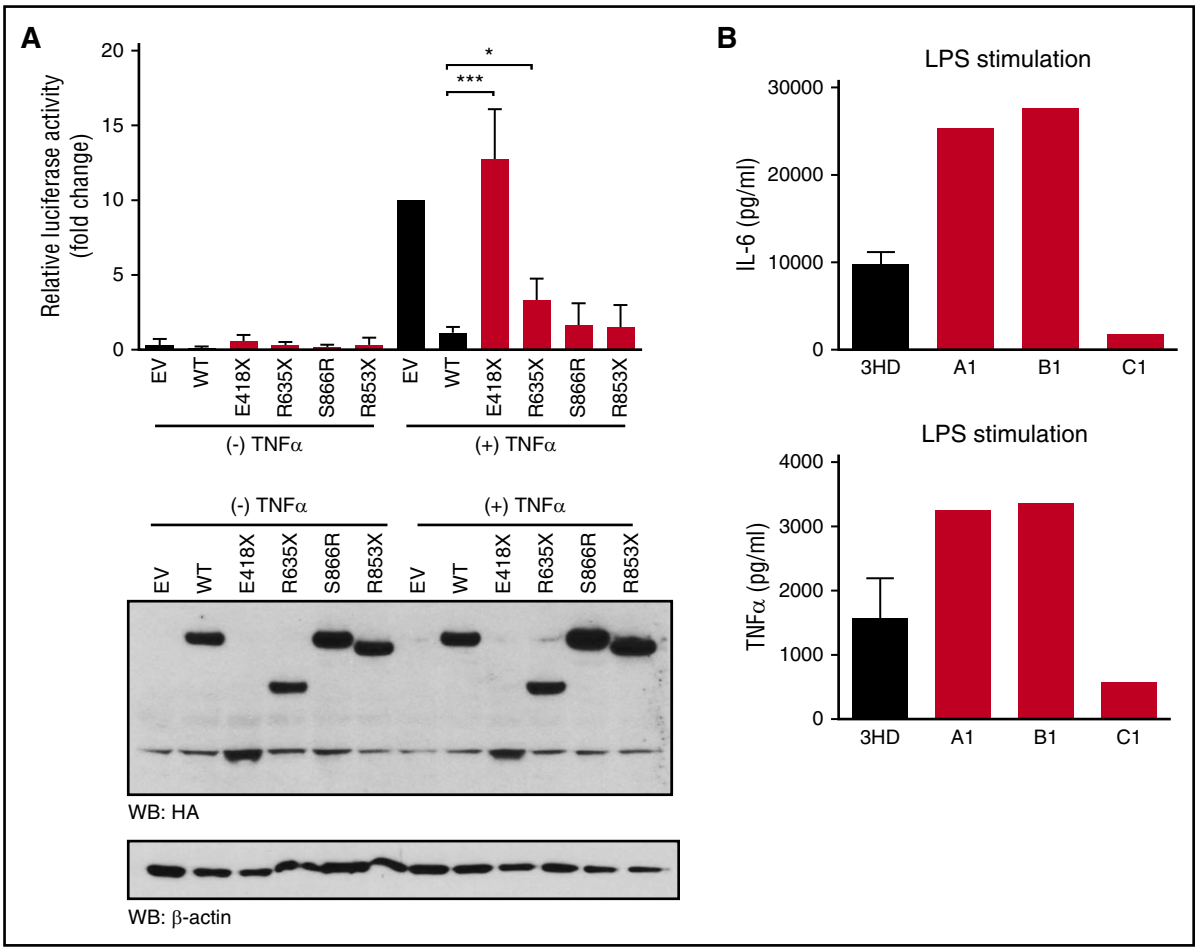

Figure 6. Increased canonical NF-κB signaling in patients with nonsense GOF *NFKB2* mutation. (A) HEK293T cells growing in 24-well plates were cotransfected with pGL4.32-NF-κB and indicated *NFKB2* expression vector. Next day, cells were treated with TNFα for 5 hours and luciferase activities were measured. Western blot analysis confirmed similar protein expression levels. The data were shown as fold change compared with TNFα-treated empty vector (pcDNA3-HA). Results shown are means + standard error of the mean of 4 experiments. **P* = .0267, ****P* = .0005 (Student *t* test). (B) Total PBMCs were stimulated with LPS (100 ng/mL) for 24 hours. Cytokine expression in supernatants was analyzed via multiplex bead assay (Luminex). Data shown are from 3 experiments with a heathy donor and indicated patients tested in pairs.

While studying genetically uncharacterized patients with PID, we found a novel C-terminal S866R dominant-negative mutation affecting 1 of the 2 NF-κB2 conserved serine residues (S866 and S870) involved in NIK- and IKKα-mediated p100 processing. This CVID patient presented with growth hormone deficiency, central adrenal deficiency, and mild ectodermal dysplasia as previously reported for other individuals carrying C-terminal *NFKB2* mutations. More interestingly, and distinct from previously described *NFKB2* mutations within the C terminus of p100, we identified 2 novel heterozygous nonsense mutations (E418X and R635X) leading to constitutively active GOF forms of NF-κB2 associated with a CID phenotype.

The NF-κB2 p100 precursor protein includes an ankyrin repeat domain (ARD) that functions as an inhibitor of NF-κB, similar to IκB. As a result, p100 interacts with RelA as well as RelB preventing activation of these proteins in response to both canonical and noncanonical stimuli.[14,23] Our work shows that mutant proteins E418X and R635X (completely or partially lacking the ARD region), but not S866R, displayed a reduced inhibitory function resulting in increased gene expression and cytokine generation upon activation of both canonical and noncanonical pathways (Figures 5C and 6B). Similar to these findings, mice carrying homozygous C-terminal ARD deletions constitutively generate active forms of p100, showing a dramatic increase in nuclear κB-specific DNA-binding activity, increased T-lymphocyte proliferation and cytokine production.[35]

Clinical and immunologic manifestations in symptomatic patients carrying the E418X and R635X GOF mutations included hypogammaglobulinemia with antibody deficiency, recurrent upper and lower respiratory bacterial infections, and lymphoproliferation, all frequently described in CVID patients. However, the patients also developed problems not characteristic of CVID including severe EBV and CMV infections, warts, mucocutaneous candidiasis, *P jirovecii* pneumonia, caseating pulmonary granulomas, lymphocytic interstitial pneumonitis, bronchiolitis obliterans, T-cell large granular lymphocyte leukemia, basal-cell carcinomas, and primary sclerosing cholangitis. Interestingly, neither endocrine abnormalities nor ectodermal dysplasia have been detected in these individuals to date. Although *NFKB2* dominant-negative mutations primarily affect NF-κB noncanonical signaling, GOF mutations affect both noncanonical and canonical NF-κB pathways. Thus, clinical differences are not surprising based on mechanistically different mutations (eg, dominant-negative vs GOF) involving a particular gene.[36-38] Whether the clinical differences are intrinsically associated with this newly described NF-κB2 GOF defect or due to a small sample bias will be determined as more patients are identified. In any case, although upregulated production of p52 is known to be associated with the development of

lymphomas in humans,[15] our study demonstrates that germ line mutations associated with upregulation of active forms of NF-κB2, as well as their loss of regulation, can detrimentally impact immune functions.

When direct relatives of our NF-κB2 GOF patients were evaluated for mutation segregation, 2 asymptomatic carriers (A2 and B3, carrying mutations E418X and R635X, respectively) were detected. Even access to blood samples and immunologic testing of the asymptomatic individuals was somehow limited, A2 showed normal lymphocyte immunophenotyping, normal NF-κB2–mediated *CXCL13* regulation, decreased p100 phosphorylation and p52 processing, and no expression of the mutant allele. In contrast, B3 had markedly reduced percent values of T cells, normal NF-κB2–mediated *CXCL13* regulation, decreased p100 phosphorylation and p52 processing, and positive expression of R635X mutant protein. Although B cells were low in all 3 of the symptomatic NF-κB2 GOF patients, they were not decreased in the 2 asymptomatic carriers. Less clear was the situation of natural killer (NK) cells as they were low in 2 of the symptomatic and 1 of the asymptomatic individuals. Altogether, these findings suggest that immunological and clinical penetrance could be incomplete and not consistently linked to *NFKB2* GOF mutations, similar to other autosomal-dominant primary immunodeficiencies recently described.[39] Moreover, although NF-κB2 is a strictly controlled immunoregulatory protein, the mechanism (s) for penetrance and expressivity for mutations resulting in GOF is still to be elucidated.

In summary, we found 3 new *NFKB2* mutations, 2 of them nonsense, resulting in GOF and leading to increased activation of both noncanonical and canonical NF-κB pathways in patients with a complex and severe immunophenotype. Taken together, our findings demonstrate that p52 plays a critical and nonredundant role in the regulation of p100/p52 protein levels and immune functions and cause a combined immunodeficiency syndrome.

Acknowledgments

The authors thank the patients and their families for their contributions to the study.

This work was supported by the Intramural Research Program, National Institutes of Health Clinical Center.

The content of this article does not necessarily reflect the views or policies of the Department of Health and Human Services, nor does mention of trade names, commercial products, or organizations imply endorsement by the US government.

Authorship

Contribution: H.S.K., T.A.F., and S.D.R. designed research, analyzed data, and wrote the paper; H.S.K., J.E.N., K.S., J.L.S., J.I., and M.P.S. performed experiments and analyzed data; and J.G., C.A.W., M.T.d.l.M., M.G., D.B.L., and C.A.S. contributed with patients to the study and analyzed data.

Conflict-of-interest disclosure: M.P.S. is a cofounder and member of the scientific advisory board of Personalis Inc, which was used for WES of one of the patients in this work. The remaining authors declare no competing financial interests.

Correspondence: Hye Sun Kuehn, Immunology Service, Department of Laboratory Medicine, NIH Clinical Center, Building 10, Room 2C306, 10 Center Dr, MSC1508, Bethesda, MD 20892; e-mail: hyesun.kuehn@nih.gov; and Sergio D. Rosenzweig, Immunology Service, Department of Laboratory Medicine, NIH Clinical Center, Building 10, Room 2C306, 10 Center Dr, MSC1508, Bethesda, MD 20892; e-mail: srosenzweig@cc.nih.gov.

References

1. Cunningham-Rundles C, Bodian C. Common variable immunodeficiency: clinical and immunological features of 248 patients. *Clin Immunol*. 1999;92(1):34-48.
2. Bogaert DJ, Dullaers M, Lambrecht BN, Vermaelen KY, De Baere E, Haerynck F. Genes associated with common variable immunodeficiency: one diagnosis to rule them all? *J Med Genet*. 2016;53(9):575-590.
3. Kuehn HS, Ouyang W, Lo B, et al. Immune dysregulation in human subjects with heterozygous germline mutations in CTLA4. *Science*. 2014;345(6204):1623-1627.
4. Schubert D, Bode C, Kenefeck R, et al. Autosomal dominant immune dysregulation syndrome in humans with CTLA4 mutations. *Nat Med*. 2014; 20(12):1410-1416.
5. Angulo I, Vadas O, Garçon F, et al. Phosphoinositide 3-kinase δ gene mutation predisposes to respiratory infection and airway damage. *Science*. 2013;342(6160): 866-871.
6. Kuehn HS, Boisson B, Cunningham-Rundles C, et al. Loss of B Cells in Patients with Heterozygous Mutations in IKAROS. *N Engl J Med*. 2016;374(11):1032-1043.
7. Picard C, Al-Herz W, Bousfiha A, et al. Primary immunodeficiency diseases: an update on the classification from the International Union of Immunological Societies Expert Committee for Primary Immunodeficiency 2015. *J Clin Immunol*. 2015;35(8):696-726.
8. Beinke S, Ley SC. Functions of NF-kappaB1 and NF-kappaB2 in immune cell biology. *Biochem J*. 2004;382(Pt 2):393-409.
9. Perkins ND. Integrating cell-signalling pathways with NF-kappaB and IKK function. *Nat Rev Mol Cell Biol*. 2007;8(1):49-62.
10. Hayden MS, Ghosh S. NF-κB in immunobiology. *Cell Res*. 2011;21(2):223-244.
11. Coope HJ, Atkinson PG, Huhse B, et al. CD40 regulates the processing of NF-kappaB2 p100 to p52. *EMBO J*. 2002;21(20):5375-5385.
12. Kayagaki N, Yan M, Seshasayee D, et al. BAFF/BLyS receptor 3 binds the B cell survival factor BAFF ligand through a discrete surface loop and promotes processing of NF-kappaB2. *Immunity*. 2002;17(4):515-524.
13. Derudder E, Dejardin E, Pritchard LL, Green DR, Korner M, Baud V. RelB/p50 dimers are differentially regulated by tumor necrosis factor-alpha and lymphotoxin-beta receptor activation: critical roles for p100. *J Biol Chem*. 2003;278(26): 23278-23284.
14. Sun SC. Non-canonical NF-κB signaling pathway. *Cell Res*. 2011;21(1):71-85.
15. Courtois G, Gilmore TD. Mutations in the NF-kappaB signaling pathway: implications for human disease. *Oncogene*. 2006;25(51):6831-6843.
16. Chen K, Coonrod EM, Kumánovics A, et al. Germline mutations in NFKB2 implicate the noncanonical NF-κB pathway in the pathogenesis of common variable immunodeficiency. *Am J Hum Genet*. 2013;93(5):812-824.
17. Liu Y, Hanson S, Gurugama P, Jones A, Clark B, Ibrahim MA. Novel NFKB2 mutation in early-onset CVID. *J Clin Immunol*. 2014;34(6):686-690.
18. Lee CE, Fulcher DA, Whittle B, et al. Autosomal-dominant B-cell deficiency with alopecia due to a mutation in NFKB2 that results in nonprocessable p100. *Blood*. 2014;124(19):2964-2972.
19. Lindsley AW, Qian Y, Valencia CA, Shah K, Zhang K, Assa'ad A. Combined immune deficiency in a patient with a novel NFKB2 mutation. *J Clin Immunol*. 2014;34(8):910-915.
20. Lougaris V, Tabellini G, Vitali M, et al. Defective natural killer-cell cytotoxic activity in NFKB2-mutated CVID-like disease. *J Allergy Clin Immunol*. 2015;135(6):1641-1643.
21. Brue T, Quentien MH, Khetchoumian K, et al. Mutations in NFKB2 and potential genetic heterogeneity in patients with DAVID syndrome, having variable endocrine and immune deficiencies. *BMC Med Genet*. 2014;15:139.
22. Shi C, Wang F, Tong A, et al. NFKB2 mutation in common variable immunodeficiency and isolated adrenocorticotropic hormone deficiency: A case report and review of literature. *Medicine (Baltimore)*. 2016;95(40):e5081.
23. Tucker E, O'Donnell K, Fuchsberger M, et al. A novel mutation in the Nfkb2 gene generates an NF-kappa B2 "super repressor". *J Immunol*. 2007; 179(11):7514-7522.
24. Shinkura R, Kitada K, Matsuda F, et al. Alymphoplasia is caused by a point mutation in the mouse gene encoding Nf-kappa b-inducing kinase. *Nat Genet*. 1999;22(1):74-77.

25. Yin L, Wu L, Wesche H, et al. Defective lymphotoxin-beta receptor-induced NF-kappaB transcriptional activity in NIK-deficient mice. *Science*. 2001;291(5511):2162-2165.

26. Michel M, Wilhelmi I, Schultz AS, Preussner M, Heyd F. Activation-induced tumor necrosis factor receptor-associated factor 3 (Traf3) alternative splicing controls the noncanonical nuclear factor κB pathway and chemokine expression in human T cells. *J Biol Chem*. 2014;289(19):13651-13660.

27. Xiao G, Harhaj EW, Sun SC. NF-kappaB-inducing kinase regulates the processing of NF-kappaB2 p100. *Mol Cell*. 2001;7(2):401-409.

28. Solan NJ, Miyoshi H, Carmona EM, Bren GD, Paya CV. RelB cellular regulation and transcriptional activity are regulated by p100. *J Biol Chem*. 2002;277(2):1405-1418.

29. Shih VF, Tsui R, Caldwell A, Hoffmann A. A single NFκB system for both canonical and non-canonical signaling. *Cell Res*. 2011;21(1):86-102.

30. Bendall HH, Sikes ML, Ballard DW, Oltz EM. An intact NF-kappa B signaling pathway is required for maintenance of mature B cell subsets. *Mol Immunol*. 1999;36(3):187-195.

31. Franzoso G, Carlson L, Poljak L, et al. Mice deficient in nuclear factor (NF)-kappa B/p52 present with defects in humoral responses, germinal center reactions, and splenic microarchitecture. *J Exp Med*. 1998;187(2):147-159.

32. Sha WC, Liou HC, Tuomanen EI, Baltimore D. Targeted disruption of the p50 subunit of NF-kappa B leads to multifocal defects in immune responses. *Cell*. 1995;80(2):321-330.

33. Fliegauf M, Bryant VL, Frede N, et al. Haploinsufficiency of the NF-κB1 Subunit p50 in Common Variable Immunodeficiency. *Am J Hum Genet*. 2015;97(3):389-403.

34. Sharfe N, Merico D, Karanxha A, et al. The effects of RelB deficiency on lymphocyte development and function. *J Autoimmun*. 2015;65:90-100.

35. Ishikawa H, Carrasco D, Claudio E, Ryseck RP, Bravo R. Gastric hyperplasia and increased proliferative responses of lymphocytes in mice lacking the COOH-terminal ankyrin domain of NF-kappaB2. *J Exp Med*. 1997;186(7):999-1014.

36. van de Veerdonk FL, Plantinga TS, Hoischen A, et al. STAT1 mutations in autosomal dominant chronic mucocutaneous candidiasis. *N Engl J Med*. 2011;365(1):54-61.

37. Dupuis S, Dargemont C, Fieschi C, et al. Impairment of mycobacterial but not viral immunity by a germline human STAT1 mutation. *Science*. 2001;293(5528):300-303.

38. Liu L, Okada S, Kong XF, et al. Gain-of-function human STAT1 mutations impair IL-17 immunity and underlie chronic mucocutaneous candidiasis. *J Exp Med*. 2011;208(8):1635-1648.

39. Conley ME, Casanova JL. Discovery of single-gene inborn errors of immunity by next generation sequencing. *Curr Opin Immunol*. 2014;30:17-23.